ACS APPLIED MATERIALS & INTERFACES

Research Article

www.acsami.org

Aminoglycoside Antibiotic-Derived Anion-Exchange Microbeads for Plasmid DNA Binding and in Situ DNA Capture

Taraka Sai Pavan Grandhi,[†] Amrita Mallik,[‡] Nan Lin,[‡] Bhavani Miryala,[‡] Thrimoorthy Potta,[‡] Yifan Tian,[§] and Kaushal Rege*[,‡]

[†]Harrington Biomedical Engineering, School of Biological and Health Systems Engineering [‡]Chemical Engineering, School for Engineering of Matter, Transport, and Energy, Arizona State University, Tempe, Arizona 85287, United States

[§]Corona del Sol High School, Tempe, Arizona 85284, United States

Supporting Information

ABSTRACT: Plasmid DNA (pDNA) therapeutics are being investigated for gene therapy and DNA vaccines against diseases including cancer, cystic fibrosis and AIDS. In addition, several applications in modern biotechnology require pDNA for transient protein production. Here, we describe the synthesis, characterization, and evaluation of microbeads ("Amikabeads") derived from the aminoglycoside antibiotic amikacin for pDNA binding and in situ DNA capture from mammalian cells. The parental aminoglycoside-derived microbeads (Amikabeads-P) acted as anion-exchange materials, and demonstrated high capacities for binding pDNA. Binding of pDNA was significantly enhanced following quaternization of the amines on the microbeads (Amikabeads-Q). Amikabeads were further employed for the disruption and extraction of DNA from mammalian cells, indicating their utility for in situ DNA capture. Our results indicate that Amikabeads are a novel material, with multiple reactive groups for further conjugation, and can have several applications in plasmid DNA biotechnology.

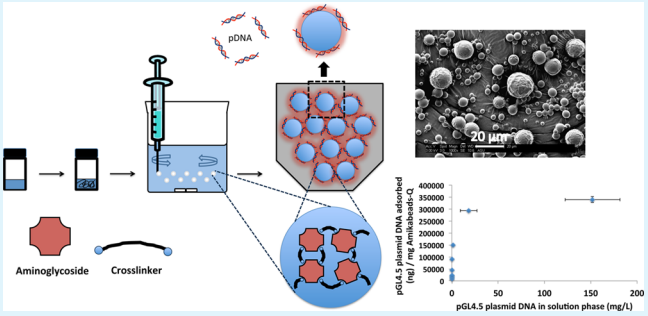

KEYWORDS: *microgel, DNA biotechnology, bioseparations, plasmid DNA binding, whole cell genomic extraction, chromatography*

1. INTRODUCTION

Plasmid DNA (pDNA)-based therapeutics are being investigated in several applications in biotechnology and medicine, including gene therapy against cancer, AIDS[1−3] and cystic fibrosis,[4] DNA-based gene vaccinations,[5] and in vitro transfections for cellular manipulation.[6] Plasmid DNA molecules are extrachromosomal pieces of double-stranded DNA[7] that confer selective advantages including antibiotic resistance in bacteria, and can be transferred to other species via horizontal gene transfer.[8,9] In cancer gene therapy, therapeutic plasmids, which code for functional tumor suppressor proteins, are delivered to cancer cells.[10] DNA-based gene vaccinations involve either direct intramuscular/intradermal injection of naked pDNA or lipid-coated delivery of the same to the target tissues.[11,12]

Plasmids are usually grown in rapidly dividing *Escherichia coli*, and can be obtained by employing different downstream purification steps. Anion-exchange chromatography,[13] affinity-based chromatography,[14] hydrophobic interaction chromatography,[15] and size-exclusion and perfusion chromatography[16] have been explored for purification of pDNA. Affinity-based chromatography methods utilize specific interactions between pDNA and surface-immobilized affinity ligands for selective binding.[17] Pseudoaffinity and affinity ligands including arginine and histidine,[18] zinc fingers,[19] LacI-LacZ moieties,[20] and triple helix forming nucleotide sequences[21] have been explored in affinity-based DNA purification approaches. Hydrophobic interaction chromatography (HIC) has also been investigated as a purification step due to differences in hydrophobicities of RNA, proteins, genomic DNA, lipopolysaccharides, and pDNA.[22,23]

Anion-exchange chromatography is widely used for pDNA chromatography, and relies on electrostatic interactions between the negatively charged backbone of pDNA and positively charged microbeads (resin).[13] For example, Q Sepharose Fast Flow resins consist of 6% cross-linked solid agarose beads that are approximately ∼90 μm in diameter. These resins, functionalized with quaternary amines, have been used for pDNA binding and purification (∼1.3 mg/mL pDNA binding capacity).[24,25] In addition, superporous/macroporous flow-through beads (e.g., POROS 50) combine high surface areas with high capacities for plasmid DNA binding and purification (∼10 mg/mL pDNA binding capacity).[25]

We have previously investigated aminoglycosides and aminoglycoside-derived materials for DNA binding and

Received: May 26, 2014
Accepted: October 14, 2014
Published: October 14, 2014

delivery.[10,26,27] Here, we report the synthesis, characterization and evaluation of novel anion-exchange microbeads (Amikabeads) derived from an aminoglycoside antibiotic, amikacin, with an eye toward applications in DNA biotechnology. Microbeads displaying quaternary amine functionalities ("Amikabeads-Q") demonstrated significantly higher pDNA binding compared to parental amikacin-derived microbeads with primary/secondary amine moieties ("Amikabeads-P"). Although high salt concentrations were effective in desorbing pDNA from Amikabeads-P, recovery of pDNA from Amikabeads-Q was greatly improved when hydrophobic modifiers (isopropyl alcohol) were included in the elution buffer. Finally, Amikabeads were also employed for mammalian cell lysis and concomitant in situ DNA sequestration directly from these cells.

2. EXPERIMENTAL SECTION

2.1. Materials. Amikacin hydrate and poly(ethylene glycol) diglycidyl ether (PEGDE) were purchased from Sigma-Aldrich Inc. (St. Louis, MO). Silicone oil and mineral oil were purchased from Acros Organics (Pittsburgh, PA). The surfactant Span-80 was purchased from TCI America (Portland, OR). Nanopure water was used for all preparations unless otherwise stated. BD Precision Glide 27G1 1/4 needles and 5 mL syringes were purchased from Becton, Dickinson and Company (Franklin Lakes, NJ). Calcein AM/ethidium homodimer-I Live/Dead stain was purchased from Life Technologies, (Carlsbad, CA). PC3 human prostate carcinoma cells were purchased from American Type Culture Collection (ATCC; Manassas, VA). Cell culture media - RPMI, Pen-Strep solution: 10 000 units/mL penicillin and 10000 μg/mL streptomycin in 0.85% NaCl solution were purchased from Hyclone (Logan, UT). A Qiagen Giga kit and Maxi kit (pDNA extraction kits) were purchased from Qiagen Inc. (Alameda, CA).

2.2. Preparation of Parental Amikagel Microbeads (Amikabeads-P). Amikabeads-P (P: parental) were generated using the emulsion polymerization method.[28] Amikacin hydrate (100 mg, 0.17 mmol) was dissolved in 1 mL of nanopure water followed by addition of poly(ethylene glycol) diglycidyl ether (PEGDE) in a mole ratio of 1:2 to generate a uniform mixture. The mixture was stirred at 100 rpm and pregelled for 4 min at 70 °C. After 4 min, the solution was collected in a syringe and dispensed slowly into a solution of mineral oil and 1% (w/v) Span-80 through 27 G1$^{1/4}$ BD PrecisionGlide needle. The mineral oil-surfactant solution was maintained at 65 °C throughout the process. Approximately ~500 μL of the pregel solution was dispensed into the heated oil phase within 25 min under constant stirring of 260 rpm. The beads were allowed to gel for 10 min after their addition followed by extensive washing and size measurements.

The beads were collected by centrifugation for 10 min at 5500 rpm. Oil was washed off the surface of the beads by using a solution of ~1% (v/v) Tween 20 detergent. Following detergent washes, the beads were finally washed multiple times with nanopure water. The particle diameters of Amikabeads-P were measured using phase-contrast microscopy; 50 beads were chosen randomly from each batch and their diameters were recorded. The averaged bead diameter of these samples was used as an indicator of size in subsequent analyses.

2.3. Formation of Amikabeads-Q by Quaternization of Amikabeads-P Microbeads. Amines and hydroxyls present in Amikabeads-P were quaternized using glycidyl trimethylammonium chloride in an aqueous solution. Excess glycidyl trimethylammonium chloride (GTMAC) was mixed with Amikabeads at 200 rpm in nanopure water for 24 h at 70 °C followed by extensive washing.[29] Quaternization was qualitatively confirmed using the ninhydrin assay,[10] as well as a fluorescein binding assay.[30] Briefly, commercially available ninhydrin reagent (200 μL) was added to 1 mg of Amikabeads-P and -Q and incubated at 99 °C for 10 min, and the color change was visually observed and recorded. For fluorescein binding studies, Amikabeads-P and -Q were incubated with 1% (v/v) NaOH solution in nanopure water for 20 min. Fluorescein sodium (200 μL of 50 mg/mL), in 1% (v/v) NaOH solution (pH > 12) made in nanopure water, was added to both bead samples. The beads were mixed with the fluorescein solution for 10 min, and then separated by centrifugation at 5000 rpm for 5 min. The beads were extensively washed with 1 mL solution of 1% (v/v) NaOH in nanopure water. The retention of fluorescein dye was visually observed and used as a qualitative indicator of quaternization.

2.4. Determination of Swelling Ratio of Amikabeads. Twenty wet Amikabeads were randomly chosen, and their diameters were measured using phase-contrast microscopy as described before. The volumes of each of these respective beads were calculated based on these diameters. The volumes of the swollen wet beads were denoted as V_{wet}. After this measurement, Amikabeads were allowed to dry at 65 °C for 24 h. Once dry, the diameters of the same beads were measured again, and their volume, V_{dry}, was calculated. The swelling ratio or SR of the beads was calculated as the following:

$$\text{SR} = \text{swollen gel volume/dry gel volume (v/v)}$$

2.5. Determination of Amikabead Amine Content. Amikabeads-P and -Q (1 mg) were freeze-dried and collected as a powder following which, 1 mL nanopure water was added to them. The ninhydrin assay reagent (100 μL) was added to 100 μL of 1 mg/mL Amikabead dispersion. The resulting solution was boiled at 99 °C for 10 min. The absorbance of the final colored solution was measured at 570 nm. The amine content was determined by comparing the absorbance of the sample solution to a calibration curve generated using glycine standards.

2.6. Total Surface Area and Porosity Estimation Using Brunauer–Emmett–Teller (BET) Method. Surface area and porosity of Amikabeads were measured via BET nitrogen sorption technique. The water in Amikabeads was gradually exchanged with acetone by suspending the beads in graded acetone series. Once the Amikabeads were soaked in 100% acetone, they were dried under vacuum before proceeding with the BET analysis. Dry Amikabeads were weighed into analytical glassware and subjected to 35 °C temperature for 11 h under constant purging with ultra high purity (UHP) nitrogen on a FlowPrep 060 Degasser. Once degassed, the sample was connected to the Micromeritics Tristar II 3020 sample port in order to carry out the experiment under vacuum in the presence of liquid nitrogen. The porosity and total surface area per mg of Amikabeads were calculated.

2.7. Scanning Electron Microscopy of Amikabeads. The surface morphology of Amikabeads was visualized using field emission scanning electron microscopy (FE-SEM; Philips FEI XL-30 SEM) at 25 kV. Amikabeads were placed on double-sided carbon adhesive tape attached on the aluminum stub, and were sputter-coated with Au–Pt for 120 s using an E1030 ion sputter. An approximately 8 nm thick Au–Pt coating was deposited on the beads on double carbon adhesive tape. SEM was performed at a voltage of 3 kV.

2.8. pDNA binding to Amikabeads. Amikabeads-P (~2 mg) were incubated with 15 000–200 000 ng of pDNA (pGL4.5) in 10 mM Tris–Cl buffer, pH 8.5 (buffer I), for 24 h at room temperature (25 °C) in order to allow pDNA binding to the beads. All Amikabeads were washed with buffer I for 6 h prior to addition of any pDNA. A NanoDrop spectrophotometer was used to measure the pDNA content in the supernatant after incubation with the beads. The amount of pDNA adsorbed onto the beads was calculated by mass balance. An adsorption isotherm was generated by calculating the amount of pDNA adsorbed on the beads at corresponding equilibrium pDNA concentrations in the supernatant. The isotherm data were fitted to a Langmuir isotherm, in order to determine the maximum binding capacity (Q_{max}) and the binding constant (K) for the Amikabeads. The Langmuir adsorption isotherm equation is shown below:

$$Q_e = \frac{(Q_{max} K C_e)}{1 + (K C_e)}$$

where Q_e = the amount of pDNA bound to the Amikabeads at equilibrium (μg/mg); C_e = concentration of pDNA in the solution at

equilibrium (mg/L); K = Langmuir adsorption constant (L/mg); Q_{max} = maximum amount of pDNA bound to Amikabeads (μg/mg).

The Langmuir equation was linearized, and $1/Q_e$ vs $1/C_e$ was plotted in order to calculate Q_{max} from the slope of the curve and the adsorption constant (K) from the intercept.

The effect of increasing salt concentration on the adsorption of pDNA on Amikabeads was also studied; 10 mM Tris−Cl was supplemented with 290 mM NaCl (buffer II), 690 mM NaCl (buffer III), and 990 mM NaCl (buffer IV), and used to allow pDNA to bind to the microbeads. The linear form of the Langmuir adsorption isotherm was used to determine parameters under these high-salt conditions as described below:

$$x = K_e C_e$$

where x = the amount of pDNA bound to 1 mg of Amikabeads (μg/mg); K_e = partition coefficient of pDNA between solution and the adsorbent (Amikabeads) (L/mg); C_e = equilibrium concentration of pDNA in the solution (mg/L).

In the case of Amikabeads-Q, 15 000−400 000 ng of pDNA was added to ∼1 mg of the quaternized beads for 24 h in 200 μL of buffer I in order to allow for binding at 25 °C. After 24 h, the static batch binding capacity of the quaternized beads was studied by determining the amount of pDNA adsorbed on to the beads, using procedures similar to those described above. The pH was maintained at 8.5 in all cases.

2.9. Visualization of pDNA Bound to Amikabeads-P and -Q. Amikabeads-P and -Q (1 mg) were incubated with 40 000 ng and 200 000 ng of pDNA in 200 μL of buffer I for 24 h at 25 °C, respectively. pDNA-Amikabead aggregates were imaged at 10× magnification using a Zeiss light microscope to measure their size. The average size of aggregates was estimated by measuring their longest length in micrometers.

Fluorescence confocal microscopy was carried out in order to visualize pDNA on the Amikabeads. After incubation of pDNA with Amikabeads for 24 h at 25 °C, 10 μM ethidium homodimer-1 was added to both Amikabeads-P and -Q for 20 min. Ethidium homodimer-I is a high-affinity nucleic acid stain that demonstrates high fluorescence upon binding to DNA, while its fluorescence is quenched in aqueous media.[31] After 20 min, the beads were separated by centrifugation, and 200 μL of Fluoro-Gel with Tris−Cl buffer (Electron Microscopy Sciences, Hatfield, PA) was added to them. The beads were mounted on a glass slide and sealed with nail polish. Ethidium homodimer-I fluorescence was observed using excitation at 514 nm, and the emission was recorded at 628 nm. The control Amikabead samples were prepared in the exact same manner, except that no pDNA was added. Adsorption of pDNA on Amikabeads was determined using a Leica SP5 confocal microscope using a 20× objective.

2.10. Desorption of Bound pDNA from Amikabeads-P and -Q. Amikabeads-P (2 mg) were loaded with 15 000−100 000 ng of pDNA in buffer I at 25 °C, in order to ensure loading in the linear as well as nonlinear portion of the adsorption isotherm. The pDNA-loaded Amikabeads-P were first washed with 200 μL of buffer I for 30 min before adding the salt solution for desorption. The amount of pDNA desorbed during the wash step was also determined. The amount of pDNA desorbed following addition of salt solutions was determined using absorbance measurements (Nanodrop) after 24 h of exposure to 1 mL of Tris−Cl buffer with 1 M salt (0.99 M NaCl and 10 mM Tris−Cl, pH 8.5) and 1 mL Tris−Cl buffer with 1.3 M salt (50 mM Tris−Cl and 1.25 M NaCl, pH 8.5) with 15% isopropyl alcohol at 25 °C. The desorption buffers were refreshed after every 24 h for Amikabeads-P until there was no further pDNA desorption from the beads.

Amikabeads-Q (1 mg) were loaded with approximately 250 000 ng of pDNA in buffer I at 25 °C; a lower amount of Amikabeads-Q was used in the desorption experiments due to the higher binding capacities of these materials. pDNA-loaded Amikabeads-Q were first washed with 200 μL of buffer I for 30 min before adding the salt solution for desorption. The amounts of pDNA desorbed were determined using absorbance measurements (Nanodrop) after 12 h of exposure to different desorption buffers at 25 °C. These included, 1 mL of Tris−Cl buffer with 1 M salt (0.99 M NaCl and 10 mM Tris−Cl, pH 8.5), Tris−Cl buffer with 1.3 M salt (50 mM Tris−Cl and 1.25 M NaCl, pH 8.5), Tris−Cl buffer with 1.3 M salt (50 mM Tris−Cl and 1.25 M NaCl, pH 8.5) supplemented with 15% isopropyl alcohol, and Tris−Cl buffer with 1.3 M salt (50 mM Tris−Cl and 1.25 M NaCl, pH 8.5) supplemented with 30% isopropyl alcohol. The desorption was also carried out at 50 °C using Tris−Cl buffer with 1.3 M salt (50 mM Tris−Cl and 1.25 M NaCl, pH 8.5) supplemented with 15% and 30% isopropyl alcohol, respectively. The desorption buffers were refreshed after every 12 h for Amikabeads-Q until there was no further pDNA desorption from the beads.

The volume of Amikabead slurry was determined in order to compare pDNA binding efficacies of Amikabeads-P and -Q microbeads with those of commercially available pDNA binding resins. It was determined that ∼1 mg of Amikabead-Q slurry had a volume of 50 μL, whereas 2 mg of Amikabead-P amounted to ∼75 μL slurry volume as prepared. The static binding capacities of Amikabeads-P and -Q resins were extrapolated to 1 mL of slurry volume, and their binding capacities were compared to commercially available resins. These analyses were carried out in order to enable a back-of-the-envelope comparison of Amikabeads with existing materials.

2.11. Agarose Gel Electrophoresis of the Desorbed pDNA. Agarose gel electrophoresis (AGE) analysis was carried out in order to investigate the integrity of the pDNA desorbed from Amikabeads. Briefly, 1 μL of pDNA (∼200 ng/μL) desorbed from the beads was mixed with 10 μL of gel loading dye (IBI 6X gel loading dye), loaded on 1% agarose gel, and run under a potential of 150 V for 30 min using 1X TAE buffer (Tris base, acetic acid, and EDTA buffer). Qualitative differences between the pDNA stock used for loading on Amikabeads, and pDNA desorbed from Amikabeads-P and -Q were visualized under ultraviolet light.

2.12. Cell Viability of PC3 Prostate Cancer Cells after Exposure to Amikabeads-P and -Q. Parental (P) and quaternized (Q) Amikabeads (100−500 μg) were added to 10 000 PC3 prostate cancer cells grown in RPMI cell culture media in 96-well plates for 24 h, in order to first determine their effect on cell viability. After 24 h, the viability of the PC3 cells was estimated using a colorimetric MTT assay in which 10 μL of MTT reagent was added to the cells for 3 h followed by detergent-mediated cell lysis. The absorbance of solubilized formazan crystals was measured at 570 nm and the background absorbance was measured at 670 nm. The resultant absorbance was used as a measure to estimate the cell viability of the PC3 prostate cancer cells.

Viability of PC3 prostate cancer cells following treatment with Amikabeads-P and -Q was also determined using the Live−Dead assay. 1 μM calcein AM and 2 μM ethidium homodimer-I in RPMI media were added to the PC3 prostate cancer cells for 20 min. After 20 min, the green fluorescence of calcein was observed using excitation: 485 ± 10 nm and emission: 530 ± 12.5 nm filter, and red fluorescence of nucleic acid bound ethidium bromide was observed using excitation: 530 ± 12.5 nm and emission: 645 ± 20 nm filter.

2.13. In Situ Sequestration of DNA from Cancer Cells Using Amikabeads. Amikabeads-P were used to induce cell lysis of PC3 human prostate cancer cells in order to facilitate extraction of cellular DNA. Amikabeads-P (100−500 μg) were added to 10 000 PC3 cells following seeding for 24 h on a 96-well plate. After 24 h of incubation, 2 μM ethidium homodimer-I was added to the cells exposed to the beads as described above. Captured genomic DNA, bound on Amikabeads-P, was visualized using fluorescence microscopy using ethidium homodimer-1.

3. RESULTS AND DISCUSSION

3.1. Generation of Microbeads (Amikabeads) Derived from an Aminoglycoside Antibiotic. Aminoglycoside antibiotics including neomycin, streptomycin, kanamycin, apramycin, and paromomycin are known to prevent growth of Gram-negative bacteria by inhibiting protein synthesis.[32] The mode of action of aminoglycoside antibiotics involves binding

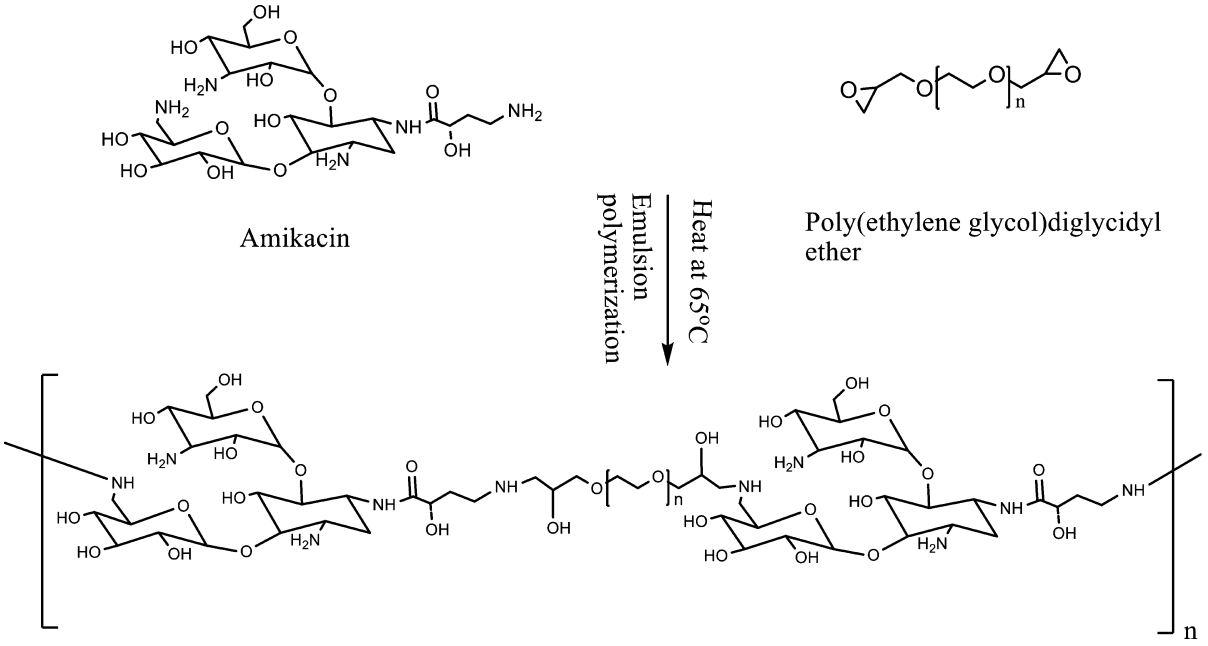

Figure 1. Schematic of the reaction between amikacin hydrate and poly(ethylene glycol) diglycidyl ether (PEGDE), resulting in the formation of Amikagel (hydrogel).

and stabilizing 16s rRNA and complexing with 30S subunit of ribosome. This, in turn, inhibits protein synthesis and causes bactericidal activity.[33] Aminoglycosides possess biocompatible sugar groups as well as multiple amines in the same molecule. Their natural affinity toward nucleic acids, makes them excellent candidates for generating diverse materials in nucleic acid biotechnology.[10,26,34] Here, we report the generation of amikacin antibiotic-derived microbeads, "Amikabeads", as anion-exchange resins for potential use in pDNA purification as well as in situ capture of DNA from mammalian cells.[35]

Reaction between amines present in amikacin with the epoxide groups in PEGDE resulted in the formation of a cross-linked hydrogel ("Amikagel"), as shown in Figure 1. It was hypothesized that multiple amines in Amikagel, particularly in the form of microbeads, can be exploited for nucleic acid (pDNA) biotechnology. Parental Amikabeads-P were generated using an emulsion polymerization method (Figure 2 a,b); a cross-linking ratio of 1:2 amikacin to PEGDE was used. The amikacin−PEGDE mixture formed a solid hydrogel within ∼8 min when stirred at 100 rpm at 70 °C. Hence, a pregelling time of 4 min was chosen, following which, the pregelled Amikagel solution was introduced into the heated mineral oil phase (65 °C, constant stirring at 260 rpm) (Figure 2). In all cases, mineral oil was supplemented with 1% Span-80 surfactant (w/v) in order to stabilize the water-in-oil microemulsion. Microbeads synthesized in absence of Span-80 were irregular, nonspherical, and appeared aggregated (Figure S1, Supporting Information).

Amikabeads-P formed in mineral oil were separated from the oil phase by centrifugation at 5000*g* for 10 min following which, the microbeads were extensively washed with nanopure water supplemented with 1% (v/v) Tween 20. Addition of Tween 20 allowed the removal of remaining Span-80 and mineral oil. Tween and Span surfactants are often mixed together in order to generate surfactants of desired Hydrophilic: Lipophilic Balance (HLB) values (Note: an HLB value of more than 10 is necessary in order to ensure surfactant solubility in water). Given the insolubility of Span-80 in water (HLB value of 4.3), Tween-20 (HLB value of 16.3) was added to solubilize and remove any remaining Span-80 and mineral oil.[36] The steps used to generate Amikabeads-P are shown in Figure 2 a,b.

3.2. Characterization of Amikabeads. *3.2.1. Shape and Particle Size of Amikabeads.* Amikabeads-P generated using the above emulsion system had spherical morphologies and demonstrated minimal aggregation (Figure 2c, Figure S1, Supporting Information), although in eventual chromatographic applications, Amikabeads will be tightly packed together as the solid phase. Amikabeads-P were sputter-coated with an 8 nm thick coating of Au−Pt in order to visualize them using scanning electron microscopy (SEM). As shown in Figure 2d, Amikagel-P microbeads had a predominantly spherical shape with smooth as well as rough surface morphology, which is similar to other hydrogel microbeads described previously.[37] The average diameter of Amikabeads-P was ∼9 ± 4 μm (Figure 2d), and was dependent on the number of times the mixture of mineral oil and span 80 was used in serial batches. Upon repeated usage of mineral oil and span 80, the diameters of Amikabeads demonstrated a modest increase ($p < 0.01$, one-way ANOVA) (Figure 3a).

We hypothesized that introduction of additional fresh Span-80 after every batch of Amikabead synthesis could limit the batch-to-batch variation in the bead size. This supplementation would account for any losses in Span-80 by thermal degradation during the preparation of each batch. As seen in Figure 3b, the diameter of Amikabeads-P did not change significantly with addition of 400 mg of fresh Span-80 after each batch of preparation. An observed *p*-value of 0.174 indicated that it is not possible to reject the null hypothesis that particle diameters in all three consecutive batches are the same in Figure 3b (*p*-value threshold of 0.05 for statistical significance). Thus, addition of Span-80 indeed reduced the batch-to-batch variation in particle diameter/size. Following this observation, we were able to mix different batches in order to obtain high amounts of Amikabeads-P for subsequent investigations.

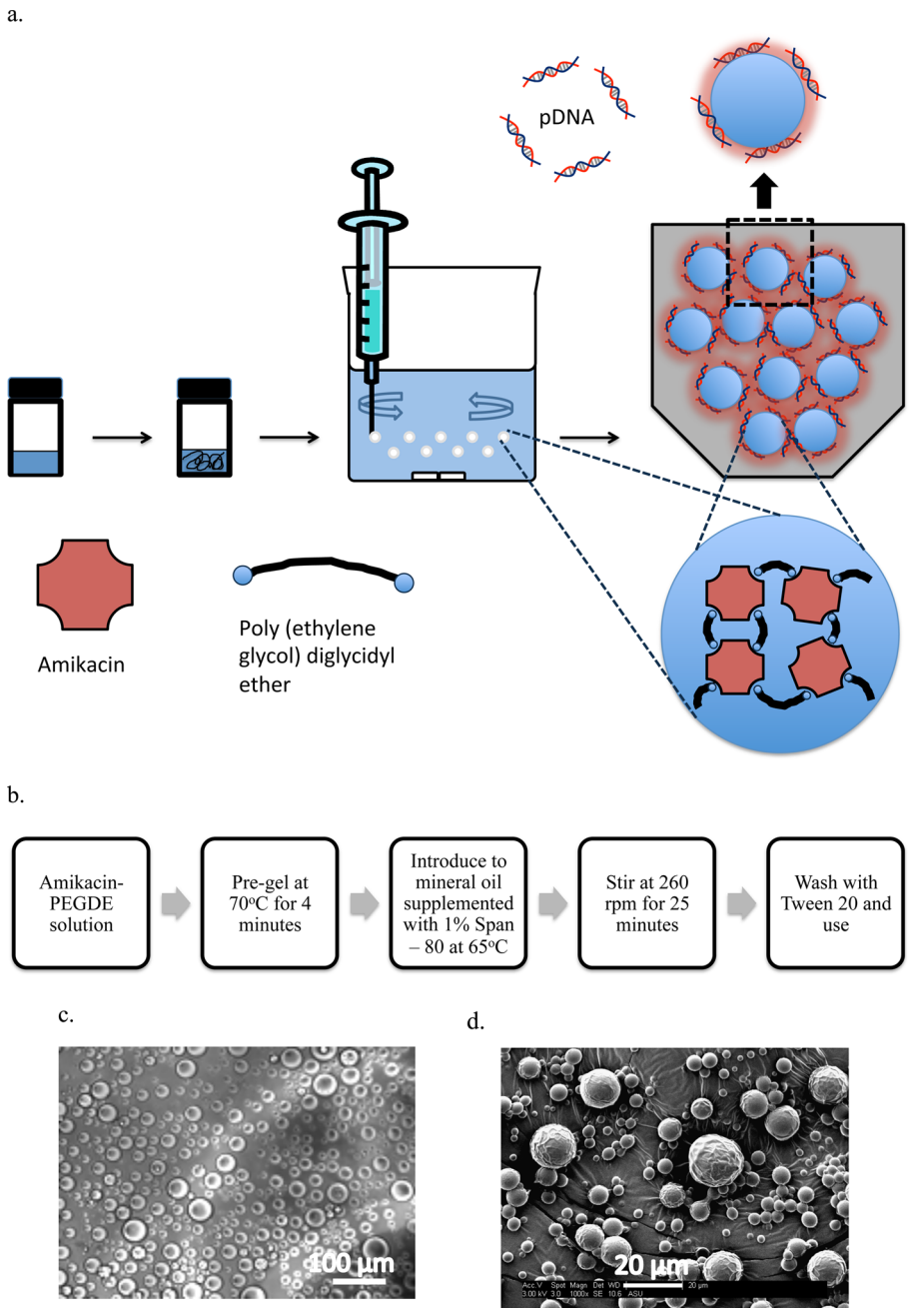

Figure 2. (a,b) Schematic of Amikabead-P synthesis. Amikabeads were prepared by pregelling the Amikagel solution for 4 min at 70 °C. The pregelled Amikagel solution was added to mineral oil bath supplemented with 1% Span-80 surfactant and maintained at 65 °C. (c) Phase-contrast image of Amikabeads-P generated after emulsion polymerization of Amikacin-PEGDE in mineral oil-1% Span-80 solution. Scale bar: 100 μm. (d) Scanning electron microscopy (SEM) image of Amikabeads indicates spherical particles with an average diameter of ~9 ± 4 μm (calculated over 50 beads).

Amikabeads-P demonstrated a swelling ratio of approximately 1.74 ± 0.2 (or 174%). This behavior is similar to commercially available anion-exchange resins, which demonstrate swelling ratios of up to 200%.[38] For example, quaternary ammonium group-containing polystyrene−divinylbenzene (PS-DVB) beads, used as strong anion exchange resins, demonstrated a swelling ratio of 1.7, which is very similar to that of Amikabeads.[39]

3.2.2. Amine Content of Amikabeads. The presence of accessible amine moieties is critical for the use of Amikabeads in anion-exchange applications. Furthermore, presence of reactive amines allows for subsequent conjugation chemistries if required. The reaction of ninhydrin reagent with reactive (primary and secondary amines) results in colorimetric changes; a bluish-purple color can be observed upon reaction with primary amines.[40] Reaction of a 0.5 mm model Amikabead with 100 μL of ninhydrin reagent at 70 °C for 10 min resulted in the formation of intense bluish-purple color throughout the bead (Figure S2, Supporting Information). The amine content of lyophilized Amikabeads-P was estimated to be 1.8 ± 0.3 μmol amine/mg of Amikabeads.

3.3. pDNA Binding to Amikabeads-P. The binding of pDNA to Amikabeads-P was determined using batch adsorption assays, in order to determine the potential use of

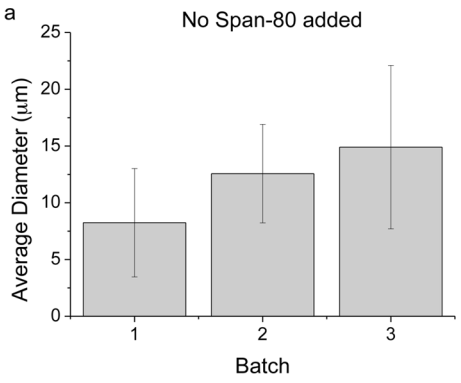

	No Span-80 added	Span-80 added
p–value of One-way ANOVA	0.00162	0.174

Figure 3. Average Amikabead-P diameter ± one standard deviation (in micrometers) of three consecutive batches (a) in absence and (b) in the presence of Span-80. The *p*-values for the one-way ANOVA test are also shown for $n = 5$ independent experiments.

these microbeads as anion-exchange resins. The pGL4.5 luciferase pDNA was used as a model plasmid in all batch binding experiments. The pGL4.5 plasmid codes for luciferase reporter protein, which is commonly used for analyzing the transfection efficacy of various nonviral vectors.[41] A Langmuir adsorption isotherm was used to fit the experimental data and obtain parameters including the maximum binding capacity (Q_{max}) and equilibrium binding constant (K). Table 1 shows the different parameters generated by fitting the experimental adsorption isotherm data to a Langmuir isotherm; the Langmuir adsorption equation was converted to its linear form in order to determine the Q_{max} value. The average ($n = 3$) maximum adsorption capacity (Q_{max}) calculated by fitting the adsorption isotherm of the Amikagel-P microbeads was approximately 44.5 μg pDNA/mg of Amikabeads-P with an equilibrium constant K of 0.04−0.06 L/mg at an equilibrium pDNA concentration (solution phase) of 300−400 mg/L. Further increasing the concentration of pDNA in the solution phase did not result in any increase in the amount of DNA adsorbed on Amikabeads-P, indicating saturation (Figure 4a, diamonds).

The pDNA binding to Amikabeads-P was significantly reduced in the presence of 0.3 M (buffer II) and 0.6 M salt (buffer III) (Table 1). As expected, higher salt concentrations screen electrostatic charges and obviate interactions between negatively charged DNA molecules and the positively charged Amikabeads-P. The saturation amount of pDNA on Amikabeads-P was not calculated under these elevated salt concentrations, because the adsorption isotherm was found to be in the linear range, even for very high pDNA concentrations in the solution phase (Figure 4a, squares).

Recovery of pDNA from Amikagels-P bound under low salt conditions (i.e., 10 mM Tris−Cl, pH 8.5) was investigated using Tris−Cl buffer with 1 M salt (0.99 M NaCl and 10 mM Tris−Cl, pH 8.5) and Tris−Cl buffer with an organic modifier (50 mM Tris−Cl and 1.25 M NaCl, with 15% isopropyl alcohol, pH 8.5). Approximately 70−100% of originally adsorbed pDNA was desorbed when a salt concentration of 1 M was used. No enhancement in desorption was observed when a buffer with higher salt concentration and isopropyl alcohol was used (Figure 4b), indicating that hydrophobic modifiers did not help recovery from Amikabeads-P. Higher percentages of desorption were observed when lesser amounts of pDNA were adsorbed onto the beads, indicating marginal losses in recovery at higher loadings (Figure 4b).

3.4. Quaternization of Amikagel-P Beads Enhances pDNA Binding. Amikacin has four primary amines, one secondary amine, and eight hydroxyl groups. It was hypothesized that quaternization of amine groups can help increase the content of positive charges in the microbeads. This, in turn, was anticipated to result in enhanced pDNA binding efficacy. The amines on the microbeads were therefore

Table 1. Langmuir Adsorption Isotherm Parameters of Plasmid DNA Binding to Amikabeads at 25 °C

ID[a]	average bead size (μm)	Q_{max} (μg/mg)	K (L/mg)	R^2
1	10 ± 3	56.0	0.01	0.97
2	11 ± 5	46.4	0.02	0.88
3	12 ± 4	31.5	0.05	0.96
ID[b]	average bead size (μm)	salt concentration (mM)	K (L/mg)	R^2
		buffer II		
1	12 ± 4	300	13.0	0.63
2	10 ± 3	300	13.2	0.71
3	10 ± 4	300	17.8	0.79
		buffer III		
4	12 ± 6	600	13.8	0.31
5	11 ± 5	600	18.3	0.27
6	10 ± 5	600	21.7	0.49

[a]Adsorption of plasmid DNA to Amikabeads-P in the presence of 10 mM Tris−Cl buffer (pH 8.5) (buffer I). [b]Adsorption of plasmid DNA to Amikabeads-P in the presence of 300 mM Tris−Cl −NaCl buffer (pH 8.5) (buffer II) and 600 mM Tris−Cl −NaCl buffer (pH 8.5) (buffer III).

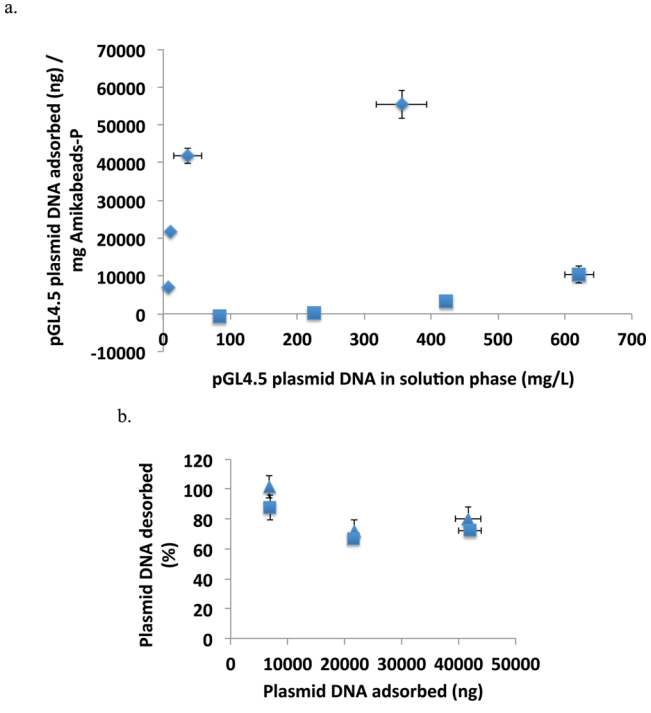

Figure 4. (a) Isotherm of pGL4.5 plasmid DNA adsorption on Amikabeads-P of diameter 11 ± 4 μm in the presence of (Buffer I) 10 mM, Tris−HCl buffer, pH 8.5, at 25 °C for 24 h (diamonds). Maximal adsorption (Q_{max}) = 44.5 μg of plasmid DNA/mg of Amikabeads-P (n = 3) (diamonds). Effect of (Buffer II) 0.3 M salt on plasmid DNA adsorption on Amikabeads of average diameter 12 ± 4 μm (squares). Reduced pDNA binding can be observed, indicating that electrostatic interactions drive adsorption. (b) Desorption of plasmid DNA from Amikabeads-P (1 mg) using Tris−Cl buffer with 1 M salt (0.99 M NaCl, 10 mM Tris−Cl, pH 8.5) after 24 h (diamonds), and Tris−Cl buffer with 1.3 M salt (1.25 M NaCl, 50 mM Tris−Cl, pH 8.5) supplemented with 15% isopropyl alcohol (squares) at 25 °C.

modified to quaternary amines using glycidyl trimethylammonium chloride (GTMAC); at neutral or acidic pH, only the amines of the amikacin react with the epoxide group of GTMAC as an addition reaction[29] (Figure S3a, Supporting Information). Formation of quaternary amines on Amikabeads was verified using both the ninhydrin assay as well as the fluorescein-binding assay. Ninhydrin reagent reacts with primary amines, resulting in the formation of a blue-purple colored product. However, as expected, quaternized Amikabeads-Q did not demonstrate a blue color, unlike unmodified Amikabeads-P (Figure S3b, Supporting Information). The fluorescein-binding assay was also able ascertain quaternization in Amikabeads-Q; in the presence of 1% (v/v) NaOH (pH > 12), the primary amines present on amikacin are no longer positively charged, whereas the quaternary amines on the quaternized beads retain the permanent positive charge. Hence, the negatively charged fluorescein can interact with and bind the quaternary ammonium moieties in Amikabeads-Q, but not the primary amines in Amikabeads-P (Figure S3c, Supporting Information).

Adsorption experiments indicated that Amikabeads-Q demonstrated significantly higher (p < 0.001) pDNA loading capacities than Amikabeads-P (Figure 5a,b). Average Q_{max} values, determined after n = 3 independent experiments, were approximately 300 μg pDNA/mg of Amikabeads-Q at an equilibrium pDNA concentration of 150−200 mg/L. This pDNA loading was approximately 30% of the weight of the Amikabeads-Q and was almost 7-fold higher than that on Amikabeads-P. It is likely that the primary amines on Amikabeads-P are only partially protonated at the pH employed in the pDNA binding studies (pH = 8.5), while the quaternary amines in Amikabeads-Q have a permanent positive charge.[42] This difference in positive charge content could partly be responsible for higher pDNA binding to Amikabeads-Q compared to Amikabeads-P.

In a recent study by Koga et al.,[43] methyl groups on a tetramethylammonium ion were found to promote hydrophilicity at a range of 0−0.08 mole fraction of the solute. Coulombic interactions between the permanent positive charge on Amikabeads-Q and the strongly anionic moieties on pDNA likely overcome the hydration of the hydrophilic quaternary amine groups on the microbeads, and result in strong pDNA-Amikabead-Q binding. Following the primary Coulombic binding, it is possible that multiple methyl groups on Amikabeads-Q participate in collective additional secondary (e.g., hydrophobic) interactions, resulting in enhanced binding to pDNA. However, the hydrophobic character/interactions is likely to be relatively modest in comparison to the high hydrophilic/cationic character imparted by quaternized amines.

Amikabeads-Q demonstrated a slightly higher average diameter than Amikabeads-P (10.8 μm for Amikabeads-P and 13.9 μm for Amikabeads-Q; Figure S4, Supporting Information). This increase in average diameter of Amikabeads-Q could be due to repulsion between the quaternized charges. However, this is likely to have a minimal contribution to the observed increase in pDNA binding capacity of Amikabeads-Q because the increase in surface area over Amikabeads-P is not significant (~1.66-fold increase in Amikabead-Q surface area over Amikabead-P surface area).

Static binding capacities of commercially available resins typically range from 1 to 10 mg of pDNA/mL of resin slurry. Gigaporous rigid ceramic HyperD-Q polymerized hydrogel resins containing quaternary amine moieties and quaternized polyethylenimine-containing porous resins (POROS HQ resins) possess among the highest static binding capacities at

a

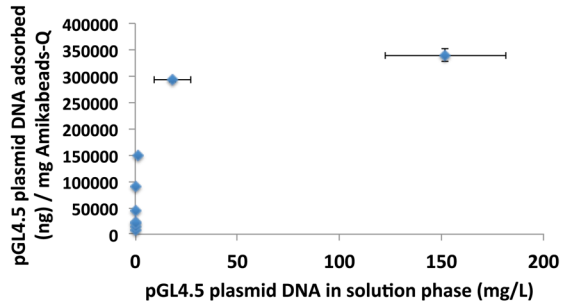

b.

Batch of Amikabeads-Q	Average Diameter (μm) ± 1 S.D (Standard Deviation)	Q_{max} DNA Binding Capacity (μg pDNA bound/mg of beads)
n=1	12 ± 6	333.3
n=2	15 ± 7	277
n=3	10 ± 6	296

c.

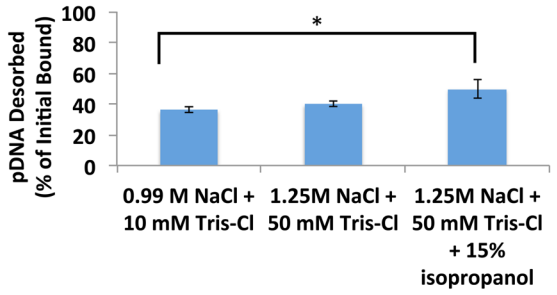

d.

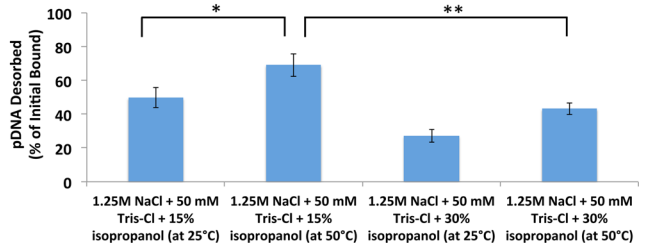

Figure 5. (a) Adsorption isotherm of pGL4.5 plasmid DNA on quaternized Amikabeads-Q (average diameter: 12 ± 6 μm) in (buffer I) 10 mM, Tris−HCl buffer, pH 8.5, at 25 °C following equilibration for 24 h. Quaternization of Amikabeads greatly enhanced the plasmid DNA binding capacity compared to Amikabeads-Q ($p < 0.001$). (b) Q_{max} calculated for three independent adsorption experiments in 10 mM, Tris−HCl buffer, pH 8.5, at 25 °C. Average Q_{max} calculated for Amikabeads-Q was ∼300 μg of plasmid DNA/mg of Amikabeads-Q. (c) Percentage of bound pDNA desorbed with Tris−Cl buffer with 1 M salt (0.99 M NaCl, 10 mM Tris−Cl, pH 8.5), Tris−Cl buffer with 1.3 M salt (1.25 M NaCl, 50 mM Tris−Cl, pH 8.5) and Tris−Cl buffer with 1.3 M salt (1.25 M NaCl, 50 mM Tris−Cl, pH 8.5) supplemented with 15% isopropyl alcohol is shown. Significantly higher desorption of pDNA was observed when isopropyl alcohol was used in the eluent ($p < 0.05$*, Students' *t*-test). (d) Desorption of pDNA from Amikabeads-Q at elevated temperature (50 °C) and higher percentage of isopropyl alcohol (30%). Increasing the temperature from 25 to 50 °C significantly improved the amount of pDNA desorbed ($p < 0.05$*, Students' *t*-test) while increasing the percentage isopropyl alcohol in the buffer from 15% to 30% had the opposite effect ($p < 0.001$**, Students' *t*-test).

∼10 mg of pDNA/mL of resin slurry.[25] Static pDNA binding capacities of Amikabeads-Q and Amikabeads-P were estimated to be ∼6 mg of pDNA/mL of resin slurry and ∼1.2 mg of pDNA/mL of resin slurry, respectively, which are comparable to that of several commercially available resins.

3.4.1. Desorption of pDNA from Amikabeads-Q. Up to 40% of bound pDNA was desorbed from Amikabeads-Q when eluted with Tris−Cl buffer containing 1 M salt (0.99 M NaCl and 10 mM Tris−Cl, pH 8.5) at 25 °C (Figure 5c). This relative desorption was significantly less in percentage than that from Amikabeads-P. Thus, although Amikabeads-Q were able to bind higher quantities of pDNA, complete recovery of the beads was not possible using 1 M salt as the elution buffer. It is known that addition of small organic molecules to desorption buffers reduces the polarity of the solution, which can facilitate desorption of molecules from resins.[44,45] Improved recovery was seen when Tris−Cl buffer containing 15% isopropyl alcohol (1.25 M NaCl and 50 mM Tris−Cl, pH 8.5) was employed for pDNA desorption at 25 °C (Figure 5c). However, use of 1.25 M NaCl did not enhance desorption of pDNA from Amikabeads-Q in absence of isopropyl alcohol (Figure 5c), indicating that the hydrophobic modifier was important for pDNA recovery from Amikabeads-Q. It is important to note that use of 15% (v/v) isopropyl alcohol did not enhance pDNA desorption from Amikabeads-P (Figure 4b), indicating that secondary hydrophobic interactions did not play a role in pDNA binding to the parental microbeads.

We observed that although use of 15% isopropyl alcohol (v/v) in the elution buffer signficantly enhanced desorption of pDNA from Amikabeads-Q, use of 30% isopropyl alcohol resulted in lower pDNA desorption from the microbeads (Figure 5d). Our results are consistent with previous observations in the literature. For example, Chang et al.[46] reported higher pDNA desorption from a substrate modified with tetraethyl quaternary ammonium groups in the presence of ∼20% isopropyl alcohol (v/v), when compared to ∼40% isopropyl alcohol (v/v). Tseng et al.[45,47] suggested the existence of a threshold volume percentage up to which the presence of an alcohol in the liquid phase can help overcome hydrophobic interactions while not greatly influencing the solution dielectric constant. This, in turn, allows for increased desorption of an adsorbed molecule from the surface, as seen in the case of pDNA desorption from Amikabeads-Q when 15% isopropyl alcohol was used in the desorption buffer. Once this threshold is crossed, increased alcohol content in the desorption buffer results in an increase in the dielectric constant of the liquid phase. This, in turn, can strengthen the magnitude of electrostatic interactions between a biomolecule and the adsorbent material. This is likely the cause for lower pDNA desroption from Amikabeads-Q when 30% isopropyl alcohol was employed in the liquid phase desorption buffer.

Finally, pDNA desorption was significantly increased when the temperature was raised from 25 to 50 °C ($p < 0.001$) (Figure 5d) in the presence of 15% isopropyl alcohol; a recovery of ∼70 ± 6% of initially adsorbed pDNA was obtained at 50 °C. Higher temperatures are known to facilitate increased desorption of pDNA from chromatographic columns,[48] and our results are along expected lines.

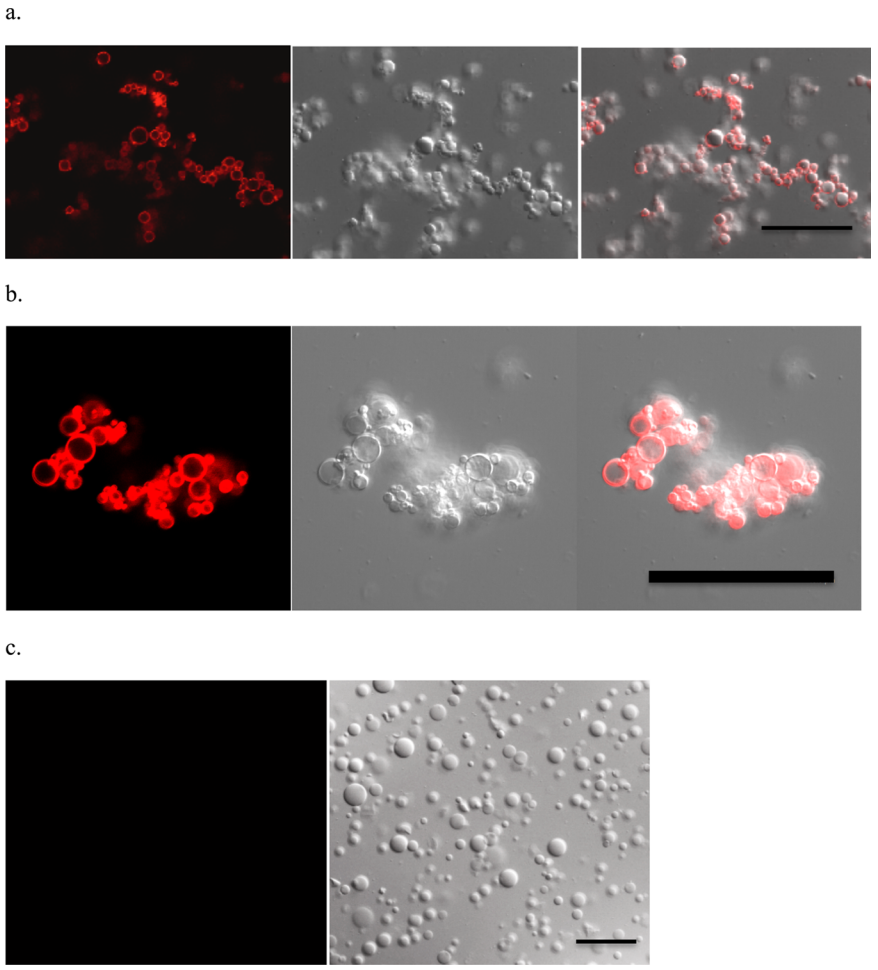

Figure 6. Confocal microscopy of pDNA loading on (a) Amikabeads-P (average diameter: ~9 ± 4 μm) and (b) Amikabeads-Q (average diameter: ~14 ± 6 μm) is shown. Amikabeads-P and -Q (1 mg each) were incubated with 40 000 ng and 200 000 ng of pDNA, respectively, in 10 mM Tris−Cl buffer, pH 8.5 at 25 °C for 24 h. Following washes, the beads were stained with 2 μM ethidium homodimer-1 for 20 min prior to imaging. Fluorescence of ethidium homodimer-1 was visualized using an excitation of 528 nm and emission of 617 nm (red color). Plasmid DNA adsorbed on the surface of both, Amikabeads-P and -Q, with minimal penetration into the beads. Amikabead clusters were observed after addition of plasmid DNA, possibly due to the bridging. (c) Amikabeads not treated with pDNA did not demonstrate ethidium homodimer-1 fluorescence and clustering. A representative image of Amikabeads-Q is shown. Scale bar = 100 μm in all cases.

The quality of the recovered pDNA from the unmodified Amikabeads-P and the quaternized Amikabeads-Q was determined by running it on a 1% agarose gel. As shown in Figure S5 (Supporting Information), the desorbed pDNA recovered by the addition of salt was of the same integrity as that of the pDNA that was loaded on the resin, indicating that Amikabeads did not induce any visible or gross damage to pDNA.

3.5. Visualization of Amikabeads before and after pDNA Binding. Confocal fluorescence microscopy was employed in order to visualize the localization of pDNA on the Amikabeads upon binding. As shown in Figure 6, pDNA was predominantly found to adsorb on the surface of both, Amikabeads-P and -Q. BET analysis indicated that Amikabeads-P possessed a surface area of approximately 2.0 m^2/g and a pore size of 4.0 nm. This pore size is consistent with that of several existing ion-exchange resins, but indicates challenges that may be associated with pDNA transport and penetration into the beads, given the larger size (70−100 nm) of supercoiled pDNA.[49] These results can explain the observation that pDNA binding is primarily observed on the surface of Amikabeads.

Amikabeads-P and -Q were found to aggregate following binding of pDNA on their surfaces, likely due to bridging of the biomacromolecule and the beads (Figure 6a,b). It is important to note that pDNA loading was in the nonlinear part of the adsorption isotherm in both cases. Neither Amikabeads-P nor Amikabeads-Q were found to aggregate in absence of pDNA loading (Figures 2c, 6c, and S6a,b, Supporting Information). The average aggregate size of pDNA with Amikabeads-Q was significantly higher than that of Amikabeads-P ($p < 0.001$, Students' t-test; Figure S6c-e, Supporting Information). It is likely that the higher cationic content on Amikabeads-Q allows the formation of bigger aggregates upon pDNA binding, compared to those seen in the case of Amikabeads-P.

Desorption of pDNA from both Amikabeads-P and -Q resulted in a decrease in aggregate size (Figure S6 f,g, Supporting Information), likey due to reduction in bridging between the biomacromolecule and the microbeads. Larger aggregate sizes were seen in the case of Amikabeads-Q compared to Amikabeads-P following desorption of pDNA. This is likely due to differences in the initial amounts of pDNA present on the microbeads, as well as in the amounts of pDNA desorbed in both cases. As described before, lower relative

amounts of pDNA were desorbed from Amikabeads-Q compared to that from Amikabeads-P (~40% of initially adsorbed pDNA for Amikabeads-Q vs ~75% of initially adsorbed pDNA for Amikabeads-P using 1 M salt). It is also possible that desorption is more challenging from Amikabeads-Q given the larger size of the aggregate first formed upon pDNA adsorption on these microbeads comapred to pDNA-Amikabead-P aggregates. This, in turn, can contribute to the higher aggregate sizes observed for Amikabeads-Q compared to those for Amikabeads-P seen after pDNA desorption (Figure S6f,g, Supporting Information).

Sizes of pDNA-Amikabead-Q aggregates following equilibration with different elution buffers were further investigated. (Figure S7a–d, Supporting Information). It was observed that, in general, the size of pDNA-Amikabead-Q aggregate decreased with increasing desorption of the biomacromolecule from the bead surface (Figure S7e, Supporting Information). Plasmid DNA that was not desorbed remained bound to the surface of Amikabeads (Figure S7f, Supporting Information). It is important to note that this colloidal aggregation behavior may be moot in cases of well-packed chromatographic columns that may employ Amikabeads as the stationary (solid) phase for biomolecule (e.g., pDNA) separations.

3.6. In Situ Capture of DNA from Mammalian Cells. Cationic microparticles and membranes have been previously used for on-site capture of genomic DNA for polymerase chain reactions.[50] For example, Cao et al.[51] reported chitosan coated beads that could extract DNA from lysed whole blood sample for PCR analyses. Here, we investigated if Amikabeads-P and -Q could be employed for extracting DNA directly from mammalian cells. PC3 human prostate cancer cells were incubated with different amounts of Amikabeads-P and -Q in order to investigate their effect on viability following cell lysis; we hypothesized that direct lysis mediated by the microbeads can facilitate extraction of DNA from cells. Amikabeads-P (500 μg, 24 h of incubation) resulted in loss of viability of ~80% of the cell population, as determined by the MTT assay (Figure 7a, diamonds). The LC_{50} (amount required to reduce cell viability to 50%) value of Amikabeads-P was approximately 400 μg for PC3 prostate cancer cells under these experimental conditions.

In contrast, unlike Amikabeads-P, Amikabeads-Q did not induce significant cell death in PC3 cells, even when amounts as high as 500 μg were employed (Figure 7b, squares). These results from the MTT assay were further confirmed using Live/Dead analyses, in concert with fluorescence microscopy (Figures 7a,b and S8, Supporting Information). Cells treated with Amikabeads-P demonstrated significantly higher levels of red fluorescence compared to those with Amikabeads-Q, because cell lysis by the former results in damage and exposure of cellular DNA to the red-fluorescent ethidium homodimer-I dye. In all cases, the microbeads were seen in close proximity with the cells (Figures 7c and S9, Supporting Information). Incubation of Amikabeads-P and -Q with PC3 cells in absence of serum proteins for 6 h did not change the toxicity of parental (P) or quaternized (Q) Amikabeads (Figure S9, Supporting Information), indicating that serum proteins have minimal or no role in determining Amikabead cytotoxicity under the conditions employed.

The above results are along the lines of previous reports in literature that indicate reduced cytotoxicity of cationic polymers after quaternization.[52−55] For example, Brownlie et al. showed that quaternization of amines in polyethylenimine (PEI)

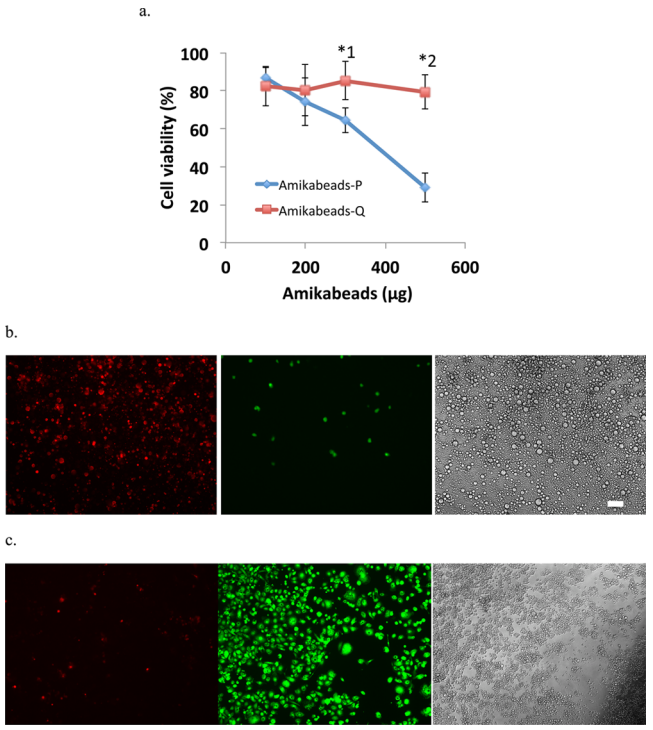

Figure 7. (a) Cell viability of PC3 human prostate cancer cells after exposure to different amounts of unmodified and quaternized Amikabeads for 24 h, as determined using the MTT assay (n = 2). *1: statistical significance p = 0.003 between cell viability of cells exposed to 300 μg of Amikabeads-P and -Q. *2: statistical significance p = 0.000 02 between cell viability of cells exposed to 500 μg of Amikabeads-P and -Q. Amikabeads-P (approximate diameter: ~12 ± 4 μm) and Amikabeads-Q (approximate diameter: ~11 ± 6 μm). Students' t-test was used to determine statistical significance. (b) Amikabeads-P (500 μg. Approximate diameter: ~12 ± 4 μm) and (c) 500 μg Amikabeads-Q (approximate diameter: ~11 ± 6 μm) were exposed to 10 000 PC3 prostate cancer cells for 24 h followed by Live (green)−Dead (red) staining. Scale bar = 100 μm. Green fluorescence emission of Calcein inside the live cells was detected using 38 HE filter set (Excitation: 470/40. Emission: 525/50) and red fluorescence of nucleic acid bound-EthD-1 was detected using a 43 HE filter set (Excitation: 550/25. Emission: 605/70).

reduced its cytotoxicity by almost 4-fold in A431 lung cancer cells.[54] Previous reports in literature[42] indicate that conversion of primary amines to quaternary amines (e.g., in the case of Amikagel-P to Amikagel-Q) results in increasing hydrophilicity of the resulting derivative. This, in turn, results in increased hydration of these molecules, which is thought to be responsible for their lower hemolytic activities.[42,55] The relatively mild negative charge on the surface of mammalian cells[56] is likely not sufficient to overcome the hydration of Amikabeads-Q (in contrast to strong Coulombic interactions of the microbeads with the strongly anionic plasmid DNA). This can likely indicate minimal interactions between the cells and Amikabeads-Q, and therefore explain the low cytotoxicity of these microbeads toward PC3 cells. However, given the lower hydration of primary amines compared to quaternary amines,[42] it is more likely for Amikabeads-P to interact with cell membranes, leading to their disruption, and eventual cell lysis. Thus, although quaternization of Amikabeads-P led to microbeads with significantly lower toxicities, Amikabeads-P were employed for directly sequestering cellular DNA following lysis of mammalian cells.

Fluorescence microscopy indicated in situ capture of cellular DNA in the case of PC3 cells treated with 12 ± 4 μm Amikabeads-P for 24 h (Figure 8a). As seen in Figure 8a,

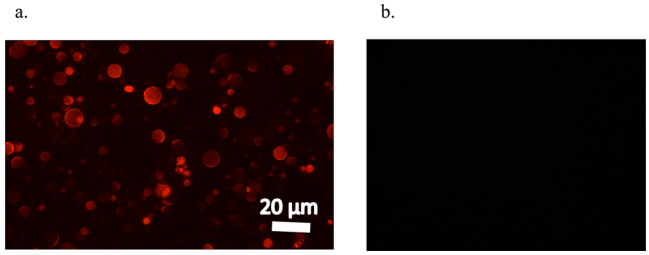

Figure 8. In situ DNA capture using Amikabeads-P from mammalian cells (a) 500 μg Amikabeads-P (approximate diameter: ~12 ± 4 μm) were exposed to 10 000 PC3 prostate cancer cells for 24 h followed by staining with the nucleic acid binding dye, ethidium homodimer-1. Nucleic acids adsorbed to the beads were stained red. (b) No red fluorescence was observed with ethidium homodimer-1 stained Amikabeads in the absence of bound DNA. Scale bar = 20 μm.

Amikabeads-P were able to simultaneously lyse cells, extract DNA molecules, and bind them. This activity of Amikabeads-P may have applications in point-of-care testing,[57] on-chip nucleic acid extraction and detection,[58] and on-site/on-chip whole cell lysis and DNA/RNA capture for PCR reactions.[59] Amikabeads-P, in absence of bound DNA, did not demonstrate any red fluorescence, which is along expected lines (Figure 8b).

4. CONCLUSIONS

We have developed a novel anion-exchange resin material based on hydrogel microbeads ("Amikabeads") generated from amikacin and poly(ethylene glycol) diglycidyl ether, with an eye toward applications in biotechnology. Parental Amikabeads-P demonstrated a Q_{max} of 44.5 μg pDNA/mg of the microbeads as determined by fitting a Langmuir isotherm to experimental batch adsorption data. Near-complete recovery of pDNA was possible from Amikabeads-P using high salt concentrations, indicating electrostatic binding between the biomolecule and the microbeads. Quaternization of amines present in parental Amikabeads resulted in the formation of microbeads (Amikabeads-Q), which demonstrated Q_{max} values approximately 7-fold higher than those for Amikagels-P under the conditions employed. Desorption of the pDNA from these beads was not as efficient as Amikabeads-P, although recovery could be significantly improved by using isopropyl alcohol as an organic modifier. Amikabeads-P were able to extract and bind cellular DNA following lysis of mammalian cells, indicating their use for in situ DNA extraction; Amikabeads-Q, however, were not able to lyse cells and demonstrated lower cytotoxicities. Our results indicate that Amikabeads are a versatile platform, with multiple easily conjugable groups for several applications in DNA biotechnology ranging from purification to cellular DNA recovery.

■ ASSOCIATED CONTENT

Supporting Information

Experimental results on ninhydrin assay of Amikabeads, quaternization procedure and characterization, agarose gels electrophoresis of pDNA, effect of desorption on pDNA-bead aggregates and PC3 cell viability results. This material is available free of charge via the Internet at http://pubs.acs.org.

■ AUTHOR INFORMATION

Corresponding Author

*Dr. Kaushal Rege. E-mail: kaushal.rege@asu.edu. Phone: (480)-727-8616. Fax: 480-727-9321.

Notes

The authors declare no competing financial interest.

■ ACKNOWLEDGMENTS

The authors thank Mr. Matt Christensen for his help with confocal microscopy, and Mr. Ashok Kumar, a graduate student at ASU for his help with SEM imaging. We also thank Dr. Joseph Chao, Center for Biosignatures Discovery Automation, Biodesign Institute, ASU, for his help with discussions regarding microbead formation. We gratefully acknowledge the National Science Foundation grant (CBET-1067840) for funding this research.

■ REFERENCES

(1) Banerjee, R.; Huang, L. Plasmid DNA–Mediated Gene Therapy. In *Burger's Medicinal Chemistry and Drug Discovery*; John Wiley & Sons, Inc.: New York, 2003; Vol. *4*, pp 641–667.

(2) Horn, N. A.; Meek, J. A.; Budahazi, G.; Marquet, M. Cancer Gene Therapy Using Plasmid DNA: Purification of DNA for Human Clinical Trials. *Hum. Gene Ther.* **1995**, *6* (5), 565–573.

(3) Anderson, W. F. Gene Therapy for Genetic Diseases. *Hum. Gene Ther.* **1994**, *5* (3), 281–282.

(4) Alton, E.; Middleton, P. G.; Caplen, N. J.; Smith, S. N.; Steel, D. M.; Munkonge, F.; Jeffery, P.; Geddes, D.; Hart, S.; Williamson, R. Non-Invasive Liposome-Mediated Gene Delivery Can Correct the Ion Transport Defect in Cystic Fibrosis Mutant Mice. *Nat. Genet.* **1993**, *5* (2), 135–142.

(5) Tighe, H.; Corr, M.; Roman, M.; Raz, E. Gene Vaccination: Plasmid DNA is More than Just a Blueprint. *Immunol. Today* **1998**, *19* (2), 89–97.

(6) Boussif, O.; Lezoualc'h, F.; Zanta, M. A.; Mergny, M. D.; Scherman, D.; Demeneix, B.; Behr, J.-P. A Versatile Vector for Gene and Oligonucleotide Transfer into Cells in Culture and In Vivo: Polyethylenimine. *Proc. Natl. Acad. Sci. U. S. A.* **1995**, *92* (16), 7297–7301.

(7) Voordouw, G.; Kam, Z.; Borochov, N.; Eisenberg, H. Isolation and Physical Studies of the Intact Supercoiled: The Open Circular and the Linear Forms of ColE1-Plasmid DNA. *Biophys. Chem.* **1978**, *8* (2), 171–189.

(8) Cohen, S. N.; Chang, A. C.; Hsu, L. Nonchromosomal Antibiotic Resistance in Bacteria: Genetic Transformation of *Escherichia coli* by R-Factor DNA. *Proc. Natl. Acad. Sci. U. S. A.* **1972**, *69* (8), 2110–2114.

(9) Elmer, J. J.; Christensen, M. D.; Rege, K. Applying Horizontal Gene Transfer Phenomena to Enhance Non-Viral Gene Therapy. *J. Controlled Release* **2013**, *172* (1), 246–57.

(10) Potta, T.; Zhen, Z.; Grandhi, T. S. P.; Christensen, M. D.; Ramos, J.; Breneman, C. M.; Rege, K. Discovery of Antibiotics-Derived Polymers for Gene Delivery Using Combinatorial Synthesis and Cheminformatics Modeling. *Biomaterials* **2014**, *35* (6), 1977–1988.

(11) Corr, M.; Lee, D. J.; Carson, D. A.; Tighe, H. Gene Vaccination with Naked Plasmid DNA: Mechanism of CTL Priming. *J. Exp. Med.* **1996**, *184* (4), 1555–1560.

(12) Hermanson, G.; Whitlow, V.; Parker, S.; Tonsky, K.; Rusalov, D.; Ferrari, M.; Lalor, P.; Komai, M.; Mere, R.; Bell, M. A Cationic Lipid-Formulated Plasmid DNA Vaccine Confers Sustained Antibody-Mediated Protection Against Aerosolized Anthrax Spores. *Proc. Natl. Acad. Sci. U. S. A.* **2004**, *101* (37), 13601–13606.

(13) Prazeres, D. M. F.; Schluep, T.; Cooney, C. Preparative Purification Of Supercoiled Plasmid DNA Using Anion-Exchange Chromatography. *J. Chromatogr. A* **1998**, *806* (1), 31–45.

(14) Sousa, F.; Prazeres, D. M.; Queiroz, J. A. Affinity Chromatography Approaches to Overcome the Challenges of Purifying Plasmid DNA. *Trends Biotechnol.* **2008**, *26* (9), 518–525.

(15) Diogo, M.; Queiroz, J.; Prazeres, D. Studies on the Retention of Plasmid DNA and *Escherichia coli* Nucleic Acids by Hydrophobic Interaction Chromatography. *Bioseparation* **2001**, *10* (4−5), 211−220.
(16) Limonta, M.; Márquez, G.; Rey, I.; Pupo, M.; Ruiz, O.; Amador-Canizares, Y.; Duenas-Carrera, S. Plasmid DNA Recovery Using Size-Exclusion and Perfusion Chromatography. *BioPharm Int.* **2008**, *21*, 38−48.
(17) Lao, U. L.; Kostal, J.; Mulchandani, A.; Chen, W. Affinity Purification of Plasmid DNA by Temperature-Triggered Precipitation. *Nat. Protoc.* **2007**, *2* (5), 1263−1268.
(18) Sousa, F.; Matos, T.; Prazeres, D.; Queiroz, J. Specific Recognition of Supercoiled Plasmid DNA in Arginine Affinity Chromatography. *Anal. Biochem.* **2008**, *374* (2), 432−434.
(19) Woodgate, J.; Palfrey, D.; Nagel, D. A.; Hine, A. V.; Slater, N. K. Protein-Mediated Isolation of Plasmid DNA by a Zinc Finger-Glutathione S-Transferase Affinity Linker. *Biotechnol. Bioeng.* **2002**, *79* (4), 450−456.
(20) Lundeberg, J.; Wahlberg, J.; Uhlén, M. Affinity Purification of Specific DNA Fragments Using a Lac Repressor Fusion Protein. *Gene Anal. Technol.* **1990**, *7* (3), 47−52.
(21) Wils, P.; Escriou, V.; Warnery, A.; Lacroix, F.; Lagneaux, D.; Ollivier, M.; Crouzet, J.; Mayaux, J.; Scherman, D. Efficient Purification of Plasmid DNA for Gene Transfer Using Triple-Helix Affinity Chromatography. *Gene Ther.* **1997**, *4* (4), 323−330.
(22) Diogo, M.; Ribeiro, S.; Queiroz, J.; Monteiro, G.; Perrin, P.; Tordo, N.; Prazeres, D. Scale-Up of Hydrophobic Interaction Chromatography for the Purification of a DNA Vaccine Against Rabies. *Biotechnol. Lett.* **2000**, *22* (17), 1397−1400.
(23) To, B.; Lenhoff, A. M. Hydrophobic Interaction Chromatography of Proteins: I. The Effects of Protein and Adsorbent Properties on Retention and Recovery. *J. Chromatogr. A* **2007**, *1141* (2), 191−205.
(24) Eon-Duval, A.; Burke, G. Purification of Pharmaceutical-Grade Plasmid DNA by Anion-Exchange Chromatography in an RNase-Free Process. *J. Chromatogr. B* **2004**, *804* (2), 327−335.
(25) Diogo, M.; Queiroz, J.; Prazeres, D. Chromatography of Plasmid DNA. *J. Chromatogr. A* **2005**, *1069* (1), 3−22.
(26) Rege, K.; Hu, S. H.; Moore, J. A.; Dordick, J. S.; Cramer, S. M. Chemoenzymatic Synthesis and High-Throughput Screening of an Aminoglycoside-Polyamine Library: Identification of High-Affinity Displacers and DNA-Binding Ligands. *J. Am. Chem. Soc.* **2004**, *126* (39), 12306−12315.
(27) Rege, K.; Ladiwala, A.; Hu, S.; Breneman, C. M.; Dordick, J. S.; Cramer, S. M. Investigation of DNA-Binding Properties of an Aminoglycoside-Polyamine Library Using Quantitative Structure-Activity Relationship (QSAR) Models. *J. Chem. Inf. Model.* **2005**, *45* (6), 1854−63.
(28) Tokuyama, H.; Yazaki, N. Preparation of Poly(*N*-isopropylacrylamide) Hydrogel Beads by Circulation Polymerization. *React. Funct. Polym.* **2010**, *70* (12), 967−971.
(29) Deveikytė, R.; Makuška, R. Quaternization of Chitosan and Partial Destruction of the Quaternized Derivatives Making them Suitable for Electrospinning. *Chemija* **2013**, *24* (4), 325−334.
(30) Tiller, J. C.; Liao, C.-J.; Lewis, K.; Klibanov, A. M. Designing Surfaces that Kill Bacteria on Contact. *Proc. Natl. Acad. Sci. U. S. A.* **2001**, *98* (11), 5981−5985.
(31) Glazer, A. N.; Peck, K.; Mathies, R. A. A Stable Double-Stranded DNA-Ethidium Homodimer Complex: Application to Picogram Fluorescence Detection of DNA in Agarose Gels. *Proc. Natl. Acad. Sci. U. S. A.* **1990**, *87* (10), 3851−3855.
(32) Kotra, L. P.; Haddad, J.; Mobashery, S. Aminoglycosides: Perspectives on Mechanisms of Action and Resistance and Strategies to Counter Resistance. *Antimicrob. Agents Chemother.* **2000**, *44* (12), 3249−3256.
(33) Mehta, R.; Champney, W. S. 30S Ribosomal Subunit Assembly is a Target for Inhibition by Aminoglycosides in *Escherichia coli*. *Antimicrob. Agents Chemother.* **2002**, *46* (5), 1546−1549.
(34) Arya, D. P.; Coffee, R. L.; Willis, B.; Abramovitch, A. I. Aminoglycoside-Nucleic Acid Interactions: Remarkable Stabilization of DNA and RNA Triple Helices by Neomycin. *J. Am. Chem. Soc.* **2001**, *123* (23), 5385−5395.
(35) Marks, M. I. In Vitro Antibacterial Activity of Amikacin, a new Aminoglycoside, Against Clinical Bacterial Isolates from Children. *J. Clin. Pharmacol.* **1975**, *15* (4), 246−251.
(36) Rodríguez, M.; Oses, J.; Ziani, K.; Mate, J. I. Combined Effect of Plasticizers and Surfactants on the Physical Properties of Starch Based Edible Films. *Food Res. Int.* **2006**, *39* (8), 840−846.
(37) Zeng, W.; Huang, J.; Hu, X.; Xiao, W.; Rong, M.; Yuan, Z.; Luo, Z. Ionically Cross-Linked Chitosan Microspheres for Controlled Release of Bioactive Nerve Growth Factor. *Int. J. Pharm.* **2011**, *421* (2), 283−290.
(38) Bodamer, G. W.; Kunin, R. Behavior of Ion Exchange Resins in Solvents other than Water-Swelling and Exchange Characteristics. *Ind. Eng. Chem.* **1953**, *45* (11), 2577−2580.
(39) Tiihonen, J.; Markkanen, I.; Laatikainen, M.; Paatero, E. Elasticity of Ion-Exchange Resin Beads in Solvent Mixtures. *J. Appl. Polym. Sci.* **2001**, *82* (5), 1256−1264.
(40) McCaldin, D. The Chemistry of Ninhydrin. *Chem. Rev.* **1960**, *60* (1), 39−51.
(41) Kean, T.; Roth, S.; Thanou, M. Trimethylated Chitosans as Non-Viral Gene Delivery Vectors: Cytotoxicity and Transfection Efficiency. *J. Controlled Release* **2005**, *103* (3), 643−653.
(42) Palermo, E. F.; Lee, D.-K.; Ramamoorthy, A.; Kuroda, K. Role of Cationic Group Structure in Membrane Binding and Disruption by Amphiphilic Copolymers. *J. Phys. Chem. B* **2010**, *115* (2), 366−375.
(43) Koga, Y.; Westh, P.; Nishikawa, K.; Subramanian, S. Is a Methyl Group Always Hydrophobic? Hydrophilicity of Trimethylamine-N-Oxide, Tetramethyl Urea and Tetramethylammonium Ion. *J. Phys. Chem. B* **2011**, *115* (12), 2995−3002.
(44) Karlström, A. E.; Hober, S. *Chromatographic Methods for Protein Purification*; Royal Institute of Technology: Stockholm, 2006.
(45) Tseng, W.-C.; Ho, F.-L. Enhanced Purification of Plasmid DNA Using Q-Sepharose by Modulation of Alcohol Concentrations. *J. Chromatogr. B* **2003**, *791* (1), 263−272.
(46) Chang, C.-S.; Ni, H.-S.; Suen, S.-Y.; Tseng, W.-C.; Chiu, H.-C.; Chou, C. P. Preparation of Inorganic−Organic Anion-Exchange Membranes and Their Application in Plasmid DNA and RNA Separation. *J. Membr. Sci.* **2008**, *311* (1), 336−348.
(47) Tseng, W.-C.; Ho, F.-L.; Fang, T.-Y.; Suen, S.-Y. Effect of Alcohol on Purification of Plasmid DNA Using Ion-Exchange Membrane. *J. Membr. Sci.* **2004**, *233* (1), 161−167.
(48) Iuliano, S.; Fisher, J.; Chen, M.; Kelly, W. Rapid Analysis of a Plasmid by Hydrophobic-Interaction Chromatography with a Non-Porous Resin. *J. Chromatogr. A* **2002**, *972* (1), 77−86.
(49) Latulippe, D. R.; Ager, K.; Zydney, A. L. Flux-Dependent Transmission of Supercoiled Plasmid DNA through Ultrafiltration Membranes. *J. Membr. Sci.* **2007**, *294* (1), 169−177.
(50) Huang, H.-C.; Barua, S.; Kay, D. B.; Rege, K. Simultaneous Enhancement of Photothermal Stability and Gene Delivery Efficacy of Gold Nanorods Using Polyelectrolytes. *ACS Nano* **2009**, *3* (10), 2941−2952.
(51) Cao, W.; Easley, C. J.; Ferrance, J. P.; Landers, J. P. Chitosan as a Polymer for pH-Induced DNA Capture in a Totally Aqueous System. *Anal. Chem.* **2006**, *78* (20), 7222−7228.
(52) Lee, J. H.; Lim, Y.-b.; Choi, J. S.; Choi, M.-u.; Yang, C.-h.; Park, J.-s. Quaternized Polyamidoamine Dendrimers as Novel Gene Delivery System: Relationship Between Degree of Quaternization and Their Influences. *Bull. Korean Chem. Soc.* **2003**, *24* (11), 1637−1640.
(53) Lee, J. H.; Lim, Y.-b.; Choi, J. S.; Lee, Y.; Kim, T.-i.; Kim, H. J.; Yoon, J. K.; Kim, K.; Park, J.-s. Polyplexes Assembled with Internally Quaternized PAMAM-OH Dendrimer and Plasmid DNA have a Neutral Surface and Gene Delivery Potency. *Bioconjugate Chem.* **2003**, *14* (6), 1214−1221.
(54) Brownlie, A.; Uchegbu, I.; Schätzlein, A. PEI-based Vesicle-Polymer Hybrid Gene Delivery System with Improved Biocompatibility. *Int. J. Pharm.* **2004**, *274* (1), 41−52.

(55) Palermo, E. F.; Kuroda, K. Chemical Structure of Cationic Groups in Amphiphilic Polymethacrylates Modulates the Antimicrobial and Hemolytic Activities. *Biomacromolecules* **2009**, *10* (6), 1416−1428.
(56) Lodish, H.; Berk, A.; Zipursky, L.; Matsudaira, P.; Baltimore, D.; Darnell, J. *Molecular Cell Biology*, 4th ed.; W. H. Freeman: New York; 2000, Section 5.3.
(57) Niemz, A.; Ferguson, T. M.; Boyle, D. S. Point-of-Care Nucleic Acid Testing for Infectious Diseases. *Trends Biotechnol.* **2011**, *29* (5), 240−250.
(58) Wu, J.; Kodzius, R.; Cao, W.; Wen, W. Extraction, Amplification and Detection of DNA in Microfluidic Chip-based Assays. *Microchim. Acta* **2013**, 1−21.
(59) Kim, J.; Johnson, M.; Hill, P.; Gale, B. K. Microfluidic Sample Preparation: Cell Lysis and Nucleic Acid Purification. *Integr. Biol.* **2009**, *1* (10), 574−586.